Low rates of nitrogen fixation in eastern tropical South Pacific surface waters

Angela N. Knapp[a,1], Karen L. Casciotti[b], William M. Berelson[c], Maria G. Prokopenko[d], and Douglas G. Capone[e]

[a]Earth, Ocean and Atmospheric Science Department, Florida State University, Tallahassee, FL 32306; [b]Department of Earth System Science, Stanford University, Stanford, CA 94305; [c]Department of Earth Sciences, University of Southern California, Los Angeles, CA 90089; [d]Geology Department, Pomona College, Claremont, CA 91711; and [e]Department of Biological Sciences, University of Southern California, Los Angeles, CA 90089

Edited by David M. Karl, University of Hawaii, Honolulu, HI, and approved February 11, 2016 (received for review August 6, 2015)

An extensive region of the Eastern Tropical South Pacific (ETSP) Ocean has surface waters that are nitrate-poor yet phosphate-rich. It has been proposed that this distribution of surface nutrients provides a geochemical niche favorable for N_2 fixation, the primary source of nitrogen to the ocean. Here, we present results from two cruises to the ETSP where rates of N_2 fixation and its contribution to export production were determined with a suite of geochemical and biological measurements. N_2 fixation was only detectable using nitrogen isotopic mass balances at two of six stations, and rates ranged from 0 to 23 μmol N m^{-2} d^{-1} based on sediment trap fluxes. Whereas the fractional importance of N_2 fixation did not change, the N_2-fixation rates at these two stations were several-fold higher when scaled to other productivity metrics. Regardless of the choice of productivity metric these N_2-fixation rates are low compared with other oligotrophic locations, and the nitrogen isotope budgets indicate that N_2 fixation supports no more than 20% of export production regionally. Although euphotic zone-integrated short-term N_2-fixation rates were higher, up to 100 μmol N m^{-2} d^{-1}, and detected N_2 fixation at all six stations, studies of nitrogenase gene abundance and expression from the same cruises align with the geochemical data and together indicate that N_2 fixation is a minor source of new nitrogen to surface waters of the ETSP. This finding is consistent with the hypothesis that, despite a relative abundance of phosphate, iron may limit N_2 fixation in the ETSP.

nitrogen fixation | eastern tropical south Pacific | nitrogen budgets | nitrate | nitrogen isotopes

Rates of marine photosynthesis significantly influence the concentration of carbon dioxide in the atmosphere, particularly on glacial–interglacial time scales (1). In broad regions of the low latitude ocean, rates of photosynthesis are thought to be limited by the availability of fixed nitrogen (N), thus restricting the biological sequestration of carbon in the deep ocean (2). The inventory of fixed N in the ocean is regulated by the balance between the principal, biologically mediated N sources and sinks, di-nitrogen (N_2) fixation, and denitrification. Despite the critical importance of the fixed N inventory in regulating photosynthesis, the spatial distribution of N fluxes to the ocean remain poorly constrained.

For decades, both geochemical and biological analyses (3–6) have pointed to a spatial decoupling of N fluxes to and from the ocean, with the highest rates of N_2 fixation documented in the tropical North Atlantic and the largest N losses concentrated in the Eastern tropical Pacific and Arabian Sea. This spatial decoupling of N inputs and outputs corresponds to a temporal decoupling, requiring the time scale of ocean circulation for N_2 fixation to respond to changes in rates of denitrification and vice versa. Despite this apparent decoupling in the modern ocean, paleoceanographic evidence indicates that N fluxes to and from the ocean have been closely balanced at least over the past 20 kyr (7, 8), although more recent work suggests transient imbalances may have occurred (9). Although N loss in the ocean is largely constrained to the sediments and water column oxygen deficient zones (ODZs) in the Eastern Pacific and Arabian Sea, similar constraints on the location of N_2-fixation fluxes to the ocean are lacking and thus the degree to which marine N sources and sinks have been coupled through time remain uncertain.

Both remote sensing (10) and biogeochemical modeling (11) have suggested that the highest rates of N_2 fixation may occur in the surface waters of the Eastern and Central tropical Pacific, which carry the geochemical signatures of N loss occurring in nearby sediments and water column ODZs (5, 6, 11). This spatial coupling of N inputs and losses in the ocean would provide the proximity necessary to allow feedbacks within the N cycle to respond to the changes in the N inventory on the decade- to hundred-year time scales apparently required by the paleoceanographic record (8, 11). Furthermore, these findings are consistent with paleoceanographic evidence for denitrification influencing the location of N_2-fixation fluxes (12). Nonetheless, these indirect estimates of high N_2-fixation rates occurring in the Eastern tropical Pacific have remained controversial in part because they challenge the well-documented high iron requirement of the enzyme nitrogenase, which carries out N_2 fixation (13, 14). The surface waters of the Central and Eastern tropical South Pacific (ETSP) receive some of the lowest atmospheric dust fluxes (15), raising the question how the largest global marine N_2-fixation fluxes (11) could occur in a region where iron sources are scarce. Indeed, previous field studies found N_2-fixation rates that were at or below detection limits and inferred that iron limits primary productivity in the region (16). Other models of the global distribution of marine N_2-fixation fluxes emphasize the iron requirements of diazotrophs and shift the bulk of predicted N_2-fixation

Significance

We present direct, field-based measurements of low nitrogen fixation rates in the eastern tropical South Pacific (ETSP) Ocean demonstrating that N_2 fixation plays a minor role supporting export production regionally. These results are in contrast to indirect estimates that the highest global rates of N_2 fixation occur in the ETSP. The low N_2-fixation rates occur in a region with relatively high surface ocean phosphate concentrations (and low nitrate concentrations) but where atmospheric iron deposition rates are diminishingly low. Consequently, these results indicate that the ETSP hosts a minor fraction of global N_2-fixation fluxes and that low nitrate to phosphate concentration ratios alone are insufficient to support high N_2-fixation fluxes.

Author contributions: A.N.K., K.L.C., W.M.B., M.G.P., and D.G.C. designed research; A.N.K., K.L.C., W.M.B., M.G.P., and D.G.C. performed research; A.N.K., K.L.C., W.M.B., M.G.P., and D.G.C. contributed new reagents/analytic tools; A.N.K., K.L.C., W.M.B., M.G.P., and D.G.C. analyzed data; and A.N.K., K.L.C., W.M.B., M.G.P., and D.G.C. wrote the paper.

The authors declare no conflict of interest.

This article is a PNAS Direct Submission.

Data deposition: The data reported in this paper have been archived in the Biological and Chemical Oceanography Data Management Office (BCO-DMO) database (hdl.handle.net/1912/7227).

See Commentary on page 4246.

[1]To whom correspondence should be addressed. Email: anknapp@fsu.edu.

This article contains supporting information online at www.pnas.org/lookup/suppl/doi:10.1073/pnas.1515641113/-/DCSupplemental.

Table 1. Results of the $\delta^{15}N$ budgets

Year and station	$\delta^{15}N_{NO3+NO2}$ (‰)	$\delta^{15}N_{PNsink}$ (‰)	f_{nfix} (%)	R_{nfix} $\delta^{15}N$ budget (μmol N m^{-2} d^{-1})	R_{nfix} short-term incub (μmol N m^{-2} d^{-1})	Short-term incubation	
						f_{nfix} (%)	$\delta^{15}N_{PNsink}$ (‰)
2010							
Station 1	11.5 ± 0.2	11.7 ± 2.1	0 ± 15	0 ± 48	37 ± 17	12	10.0
Station 3	11.1 ± 0.01	13.7	0	0 ± 0	98 ± 129	362	−1
Station 5	9.8 ± 0.9	11.1 ± 0.1	0 ± 0	0 ± 0	51 ± 20	170	−1
2011							
Station 1	11.8 ± 0.1	9.2 ± 1.4	21 ± 10	24 ± 13	23 ± 24	20	9.2
Station 5	10.1 ± 0.0	7.9 ± 2.1	20 ± 19	11 ± 10	86 ± 9	160	−1
Station 13	9.6 ± 0.9	13.2 ± 2.3	0 ± 0	0 ± 0	61 ± 22	39	5.4

Results include $\delta^{15}N_{NO3+NO2}$ end-member (±1 SD), measured $\delta^{15}N_{PNsink}$ (±1 SD), the calculated fractional contribution of N_2 fixation to export production (f_{nfix}; %) (±1 SD), and N_2-fixation rate (R_{nfix} $\delta^{15}N$ budget; μmol N m^{-2} d^{-1}) (±1 SD), as well as N_2-fixation rates from short-term $^{15}N_2$ incubations (R_{nfix} short-term incub; μmol N m^{-2} d^{-1}) (±1 SD). The last two columns report the fraction of the PN_{sink} flux that would be supported by N_2 fixation as well as the $\delta^{15}N_{PNsink}$ that would be expected assuming the short-term N_2-fixation rate; see *Discussion* for details.

fluxes to the Southwest Pacific Ocean proximal to larger atmospheric dust sources (17–19).

Given the uncertainty in the spatial distribution of N_2 fixation in the global ocean, field campaigns making direct measurements of N fluxes to the ocean remain a priority, in particular in the expansive ETSP gyre, where few such measurements have been made (20). Here, we present a suite of measurements from the ETSP gyre, collected between 80°W to 100°W along 20°S (Fig. S1), evaluating N_2 fixation on ∼1- to 3-d time scales, including short-term (i.e., 24 h) $^{15}N_2$ incubation-based fixation rates. N_2-fixation rates and their contribution to export production were also evaluated with a N isotope mass balance which compared the isotopic composition of sinking particulate N (PN_{sink}) collected for 35–70 h in floating sediment traps with that of subsurface NO_3^-. Together with a parallel analysis of the abundance and expression of the dinitrogenase reductase iron protein encoded by the *NifH* gene from the same cruises (21), as well as measurements of the isotopic composition of PN_{sink} collected over 13 mo in a deep-moored sediment trap (22), these datasets constrain the role of N_2 fixation in the ETSP gyre.

Results

N_2-Fixation Rates and Their Contribution to Export Production in the ETSP. N_2-fixation rates calculated with geochemical methods track the distinct imprints that diazotrophs leave on water column nutrient stoichiometry and isotopic composition. The approach used here relies on the unique isotopic signature ($\delta^{15}N = \{[(^{15}N/^{14}N)_{sample}/(^{15}N/^{14}N)_{reference}] - 1\} \times 1{,}000$, with atmospheric N_2 as the reference) of diazotrophic biomass [$\delta^{15}N_{Nfix}$ = −2–0‰ (23, 24)], which is low compared with that of mean ocean nitrate [$\delta^{15}N_{NO3}$, ∼5‰ (25)]. Because the $\delta^{15}N$ of the two dominant sources of new N to surface waters [subsurface NO_3^- + nitrite (NO_2^-) and N_2 fixation] have distinct $\delta^{15}N$ values, the $\delta^{15}N$ of these two sources can be used together with the $\delta^{15}N$ of PN_{sink} ($\delta^{15}N_{PNsink}$) to construct a two end-member mixing model ($\delta^{15}N$ budget) to estimate the relative importance of each for supporting export production (26–28) (Fig. S2). The fractional importance of N_2 fixation for supporting export production (x) can be expressed as

$$\delta^{15}N_{PNsink} = x\left(\delta^{15}N_{Nfix}\right) + (1-x)\left(\delta^{15}N_{NO3+NO2}\right). \quad [1]$$

Rearranging and solving for x yields

$$x = \left(\delta^{15}N_{NO3+NO2} - \delta^{15}N_{PNsink}\right) / \left(\delta^{15}N_{Nfix} + \delta^{15}N_{NO3+NO2}\right). \quad [2]$$

Multiplying x by the PN_{sink} flux provides a time-averaged N_2-fixation rate that can be compared with short-term N_2-fixation rate measurements.

Floating sediment trap $\delta^{15}N_{PNsink}$ and water column $\delta^{15}N_{NO3+NO2}$ measurements from two cruises to the ETSP (January to February 2010 and March to April 2011) were used to construct the $\delta^{15}N$ budgets (Table 1 and Fig. S1). This approach depends on the careful characterization of both the $\delta^{15}N_{Nfix}$ as well as the $\delta^{15}N_{NO3+NO2}$ end-members. The $\delta^{15}N_{Nfix}$ end-member is constrained by field measurements of diazotrophic biomass $\delta^{15}N$ that range between approximately −2‰ and 0‰ (23, 24); lower $\delta^{15}N_{Nfix}$ values result in a lesser contribution of N_2 fixation to export production (Eq. **2**). Here, we take $\delta^{15}N_{Nfix} = -1‰$. Uncertainty in the $\delta^{15}N_{NO3+NO2}$ end-member largely depends on the degree to which $\delta^{15}N_{NO3+NO2}$ varies with depth in the upper thermocline and whether or not there is unconsumed $NO_3^- + NO_2^-$ in surface waters. At these stations, mixed layer concentrations of $NO_3^- + NO_2^-$ were typically at or below detection limits (0.05 μM) (except in 2011 at the more northern Station 13, where the mixed-layer $NO_3^- + NO_2^-$ concentration was between 0.3 and 0.6 μM) and increased rapidly below the base of the euphotic zone (Fig. 1 and Table S1). Effectively complete consumption of surface water $NO_3^- + NO_2^-$ in this region of the ETSP alleviates concerns with the choice of isotope effect used for NO_3^- assimilation in $\delta^{15}N$ budget calculations (29, 30). Profiles at eastern stations (i.e., Stations 1 and 13) show isotopic features indicative of dissimilatory NO_3^- reduction occurring in the nearby ODZs of the ETSP (Fig. 1) (6, 31–33). Additional increases in $\delta^{15}N_{NO3+NO2}$ coincident with the deep chlorophyll *a* maximum (Stations 1, 3, and 13; Fig. 1) indicate that NO_3^- assimilation elevated the $\delta^{15}N_{NO3+NO2}$ within and immediately below the base of the euphotic zone (34, 35).

Because the ETSP has strong gradients in $\delta^{15}N_{NO3+NO2}$ with depth in the upper thermocline (31, 33), we use water column profiles of density, $NO_3^- + NO_2^-$ concentration, and $\delta^{15}N_{NO3+NO2}$, together with fluorescence (2010 cruise) or chlorophyll *a* concentration (2011 cruise), to select the $\delta^{15}N_{NO3+NO2}$ end-member at each station (Fig. 1 and Table S1). The $\delta^{15}N$ budgets were evaluated with three choices of the $\delta^{15}N_{NO3+NO2}$ end-member: (*i*) the deep chlorophyll maximum, (*ii*) the depth of the floating sediment trap, and (*iii*) the shallowest $\delta^{15}N_{NO3+NO2}$ minimum (Table S2). The lower concentration and elevated $\delta^{15}N_{NO3+NO2}$ at the base of the deep chlorophyll maximum relative to depths immediately below (Fig. 1) indicates that NO_3^- assimilation has affected the $\delta^{15}N_{NO3+NO2}$ at this depth and that the source of $NO_3^- + NO_2^-$ to the euphotic zone has a lower $\delta^{15}N$, arguing against this choice for the $\delta^{15}N_{NO3+NO2}$ end-member (36). A similar argument can be made against assigning a $\delta^{15}N_{NO3+NO2}$ source at the depth of the sediment trap. We argue that the shallowest $\delta^{15}N_{NO3+NO2}$ minimum is most representative of the unaltered source of $NO_3^- + NO_2^-$ to the euphotic zone. Similar to the $\delta^{15}N_{Nfix}$ end-member choice, lower

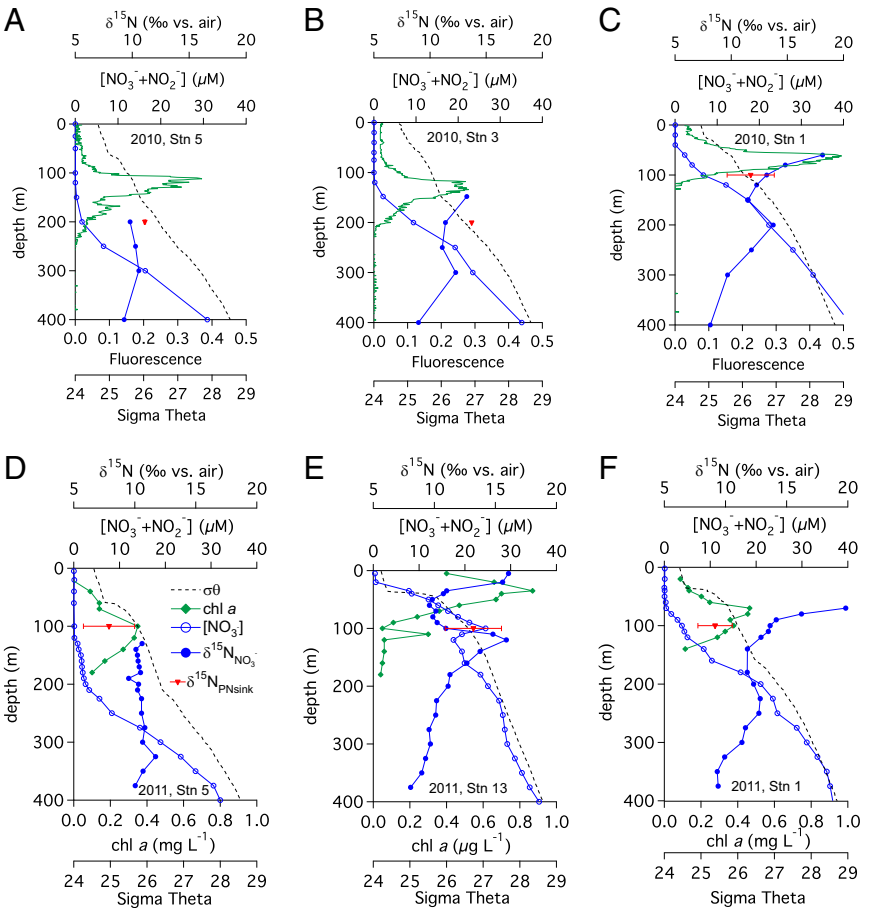

Fig. 1. Biogeochemical characterization of the ETSP upper thermocline. Water column profiles of potential density (dashed black line), $NO_3^- + NO_2^-$ concentration (open circles), $\delta^{15}N_{NO3+NO2}$ (filled circles), $\delta^{15}N_{PNsink}$ with error bars (±1 SD) (filled triangles), and CTD fluorescence trace from the 2010 cruise (solid green line) or discrete chlorophyll *a* measurements from the 2011 cruise (filled diamonds) for 2010 Station 5 (100°W, 20°S) (*A*), 2010 Station 3 (90°W, 20°S) (*B*), 2010 Station 1 (80°W, 20°S) (*C*), 2011 Station 5 (100°W, 20°S) (*D*), 2011 Station 13 (82°W, 15°S) (*E*), and 2011 Station 1 (80°W, 20°S) (*F*).

$\delta^{15}N_{NO3+NO2}$ end-member values will result in a smaller role for N_2 fixation in supporting export production (Eq. **2**). For comparison, the results of all three approaches are given in Table S2.

On the 2010 cruise, which took place during the austral summer from January to February 2010, the $\delta^{15}N$ budgets did not detect N_2 fixation at any of the three stations (Table 1 and Fig. S1). However, at Station 1, the SD associated with the $\delta^{15}N_{PNsink}$ measurement (11.7 ± 2.1‰) leads to relatively high uncertainty in the N_2-fixation rate, 0 ± 48 μmol N m^{-2} d^{-1}, leaving open the possibility that N_2 fixation may have contributed up to 15% of export production (Table 1). At Station 3, no replicate measurements of the $\delta^{15}N_{PNsink}$ (13.7‰) were made, so no uncertainty in the N_2-fixation rate of 0 μmol N m^{-2} d^{-1} could be estimated. At Station 5, the low SD associated with the $\delta^{15}N_{PNsink}$ measurement (11.1 ± 0.1‰) corresponds to no range in either the fractional contribution of N_2 fixation to export production (0 ± 0%) or the N_2-fixation rate (0 ± 0 μmol N m^{-2} d^{-1}) (Table 1).

In March to April 2011, N_2 fixation was detected in the $\delta^{15}N$ budgets at Stations 1 and 5 (Table 1 and Fig. S1). The $\delta^{15}N$ budget at Station 1 gave an N_2-fixation rate of 24 ± 13 μmol N m^{-2} d^{-1}, supporting 21 ± 10% of export production, which appears somewhat high and inconsistent with the lack of molecular evidence for diazotrophs at this station (21). Despite the relatively high SD of duplicate $\delta^{15}N_{PNsink}$ measurements (9.2 ± 1.4‰), the range of $\delta^{15}N_{PNsink}$ values within the uncertainty are lower than all of the $\delta^{15}N_{NO3+NO2}$ shallower than 350 m (Fig. 1 and Table S1), indicating that N_2 fixation is the likely source of the low-$\delta^{15}N$ N required to balance the $\delta^{15}N$ budget at Station 1. In addition, the $\delta^{15}N$ mass balance-based N_2-fixation rate is indistinguishable from the short-term N_2-fixation rate measured at this station in 2011 (see *Discussion* below) (Table 1).

The $\delta^{15}N_{PNsink}$ at Station 5 on the 2011 cruise was 7.9 ± 2.1‰, lower than the $\delta^{15}N_{NO3+NO2}$ throughout the upper 400 m, which is relatively constant with depth compared with other stations (Fig. 1). The $\delta^{15}N$ budget at Station 5 yields N_2-fixation rates of 11 ± 10 μmol N m^{-2} d^{-1}, supporting 20 ± 19% of export production, although we note that the very low mass flux (0.05 mmol N m^{-2} d^{-1}) (Table S3) likely contributes to the large uncertainty in $\delta^{15}N$ budget calculations. The $\delta^{15}N_{PNsink}$ at Station 13 was 13.2 ± 2.3‰, which is higher than the $\delta^{15}N_{NO3+NO2}$ at the shallowest $\delta^{15}N_{NO3+NO2}$ minimum, 9.6 ± 0.9‰, and thus implies that N_2 fixation does not support any export production at this station. However, a higher $\delta^{15}N_{PNsink}$ than the $\delta^{15}N_{NO3+NO2}$ end-member indicates that another $\delta^{15}N_{NO3+NO2}$ end-member may be more appropriate. For example, up to 16 ± 13% of export production at Station 13 could be supported by N_2 fixation if 100% of the $NO_3^- + NO_2^-$-fueled export production at this station originated between 100 and 150 m, with a maximum $\delta^{15}N_{NO3+NO2}$ of 15.9‰, and where a secondary peak in chlorophyll *a* was observed (Fig. 1).

N_2-Fixation Rates Derived from Productivity Metrics. In the regions of the ETSP with NO_3^--depleted surface waters, the $\delta^{15}N_{PNsink}$ flux is more similar to the $\delta^{15}N_{NO3+NO2}$ in the upper thermocline

than to the $\delta^{15}N_{Nfix}$ end-member (Fig. 1), indicating that $NO_3^- + NO_2^-$ is the dominant source of new N fueling export production, consistent with results from other regions with NO_3^--depleted surface waters (26–28). Although the composition of material captured in surface-tethered floating sediment traps is considered representative of the sinking flux, the magnitude of the export flux determined by sediment traps was lower than that recorded by other metrics of new and export production on these two cruises (37), as has been found previously (38). In cases where the $\delta^{15}N$ budgets fail to detect N_2 fixation, multiplying by alternative productivity metrics would not yield positive N_2-fixation rates, and we expect that the results of the $\delta^{15}N$ budgets that fail to detect N_2 fixation at four of the six stations are robust (see *Discussion* below). However, when N_2 fixation is detected in the $\delta^{15}N$ budgets, multiplying the fraction of export production supported by N_2 fixation (x in Eq. **1**) by an underestimate of the export flux may consequently underestimate N_2-fixation rates.

To address potential underestimation of N_2-fixation rates attributable to undercollection of the export flux by the sediment traps, N_2-fixation rates were also calculated using alternative metrics of new production (O_2/Ar ratios, ^{14}C uptake) and export production (^{234}Th deficits) (Table S4). These alternative productivity metrics yielded higher rates of N_2 fixation, with the highest N_2-fixation rates at Station 1 resulting from multiplying the fractional importance of N_2 fixation by the O_2/Ar-based net community production (NCP) estimate (197 ± 59 μmol N m^{-2} d^{-1}) and at Station 5 by the ^{234}Th-deficit estimate of export production (100 ± 30 μmol N m^{-2} d^{-1}). Multiplying the fractional contribution of N_2 fixation to export production by these alternate productivity metrics provides a geochemically derived upper bound to regional N_2-fixation rates, which, although lower than rates from the tropical North Atlantic (4), are comparable to the intermediate rates observed in the summer in the North Pacific gyre (39). Although this study did not extend to the regions of the Central Pacific, where N_2 fixation was diagnosed by remote sensing studies (10), the prediction for the favorable surface ocean NO_3^- and PO_4^{3-} concentrations and stoichiometry in the ETSP gyre to support the highest global N_2-fixation fluxes (11) is not supported by $\delta^{15}N$ budget calculations.

Discussion

Despite the $\delta^{15}N$ budgets only detecting N_2 fixation at Stations 1 and 5 on the 2011 cruise, N_2 fixation was detected by short-term rate measurements at all stations on both cruises (Table 1). In 2011, the short-term N_2-fixation rate at Station 1 (23 ± 24 μmol N m^{-2} d^{-1}) is indistinguishable from the $\delta^{15}N$ budget-based rate using sediment trap fluxes (24 ± 13 μmol N m^{-2} d^{-1}), but lower than the other geochemical N_2-fixation flux estimates, which range from 111 to 197 μmol N m^{-2} d^{-1} (Table S4). At Station 5, the short-term rate (86 ± 9 μmol N m^{-2} d^{-1}) is higher than all but the ^{234}Th-based N_2-fixation rate estimate, 100 ± 30 μmol N m^{-2} d^{-1} (Table S4). To evaluate whether the short-term N_2-fixation rates are consistent with the $\delta^{15}N$ measurements, we (*i*) compare short-term rates of N_2 fixation with the PN_{sink} mass flux (Table S3) to evaluate what fraction of the PN_{sink} flux the short-term rate represents ("f_{nfix}") and (*ii*) calculate what the $\delta^{15}N_{PNsink}$ would need to be for the $\delta^{15}N$ budget to match the short-term rates (Table 1).

As described above, the $\delta^{15}N$ budget-based N_2-fixation rate is indistinguishable from the short-term incubation results at Station 1 in 2011, resulting in a predicted $\delta^{15}N_{PNsink}$ identical to what was measured (Table 1). At Station 13 in 2011, the short-term rates correspond to 39% of the export flux and would have resulted in a $\delta^{15}N_{PNsink}$ of 5.4‰, significantly lower than the measured $\delta^{15}N_{PNsink}$ of 13.2 ± 2.3‰ (Table 1). At the stations with lower organic matter fluxes, the short-term N_2-fixation rates were several-fold larger than the PN_{sink} fluxes (2010 cruise, Stations 3 and 5, and 2011 cruise Station 5), corresponding to predicted $\delta^{15}N_{PNsink}$ values of −1‰ (Table 1). We note that the discrepancy at Stations 3 and 5 on the 2010 cruise is exacerbated by the collection of the PN_{sink} flux at 200 m; at all other stations, the PN_{sink} flux was collected at 100 m (Table S3). At Station 5 in 2011, we suspect that the low mass flux at this ultraoligotrophic station (16), with the high SD for $\delta^{15}N_{PNsink}$, contributes to the larger discrepancy between the short-term N_2-fixation rate and the PN_{sink} flux. We also note that the calculation of f_{nfix} with the PN_{sink} flux, as opposed to the other metrics of new and export production, represents an upper limit to the fractional importance of N_2 fixation for supporting export production. However, together, these calculations suggest that the short-term N_2-fixation rates should have been apparent in all of the $\delta^{15}N$ budgets.

The larger discrepancy between the $\delta^{15}N$ budget- and short-term incubation-based N_2-fixation rates at stations with lower PN_{sink} fluxes requires consideration of potential explanations. First, the N_2 fixation measured in the short-term incubations may not have contributed to sinking particles if the diazotrophs did not sink and/or were grazed and not converted to fecal pellets before the sediment traps were recovered. However, this scenario might be expected to correspond to a stronger quantitative PCR-based signal of *NifH* than was observed at these stations (21) (see below). Additionally, analysis of $\delta^{15}N_{PNsink}$ collected at Station 5 in a deep (i.e., 3,660 m), moored sediment trap deployed from February 2010 to March 2011 shows that the $\delta^{15}N_{PNsink}$ does record the input of low-$\delta^{15}N$ material, and thus N_2 fixation's geochemical signature is most pronounced, during the austral summer, when mass fluxes were lowest (22). Moreover, there is no evidence for preferential remineralization of low-$\delta^{15}N$ material between the surface-tethered and 3,660-m traps (22), suggesting that whatever low-$\delta^{15}N$ PN_{sink} material was produced in surface waters was not rapidly remineralized to low-$\delta^{15}N$ NO_3^- in the upper thermocline, as may occur in the subtropical North Pacific (28) and North Atlantic gyres (35), where N_2-fixation rates are higher. Finally, euphotic zone DON concentration and $\delta^{15}N$ at these stations (~4.5–5.0 μM and 5.0 ± 0.5‰) were consistent with previous measurements from the North Pacific (40) and did not indicate that newly fixed N accumulated in the surface DON pool.

Another potential explanation for the discrepancy between the geochemical and short-term N_2-fixation rates comes from recent work documenting the presence of ^{15}N-labeled N-oxides and/or ammonium (NH_4^+) in several brands of $^{15}N_2$-labeled gas (41), which could lead to an overestimate of N_2-fixation rates using $^{15}N_2$ tracer techniques, especially when N_2-fixation rates are low, as in the ETSP. Short-term N_2-fixation rates in this study were determined using two (2010 cruise) or three (2011 cruise) different brands of $^{15}N_2$ labeled gas, including those identified as more and less contaminated (41), and showed largely comparable rates and many instances of N_2-fixation rates at or near the limit of detection, arguing against this explanation as the cause of the discrepancy. Indeed, other work argues that short-term rates determined with $^{15}N_2$ gas may underestimate N_2-fixation rates if $^{15}N_2$ gas is not properly equilibrated before incubation (42), which, if correct, would exacerbate the difference between short-term and geochemical N_2-fixation rate estimates in this study.

The $\delta^{15}N$-budget– and short-term incubation-based N_2-fixation rate estimates integrate over 24- to 70-h periods; in the context of the offset between the geochemical and short-term N_2-fixation rates, it is useful to consider the results from a study of *NifH* gene expression on these same cruises, which should reflect diazotrophic activity over comparable time scales (21). Although diazotrophs could be detected, their abundance and activity in the ETSP was low compared with studies from other oligotrophic regions (21). Moreover, the heterotrophic diazotrophs that dominated the diaozotrophic community in the ETSP gyre typically have significantly lower per-cell N_2-fixation rates than the

cyanobacterial diazotrophs common where higher N_2-fixation rates are found (4, 21, 39), and these low per-cell rates could not be reconciled with previously reported short-term N_2-fixation rates in the ETSP gyre (21, 43). Thus, the molecular results from these cruises are consistent with the results of the $\delta^{15}N$ budgets that fail to detect significant rates of N_2 fixation at four of the six stations in the ETSP. The discrepancy between the *NifH* results and the short-term N_2-fixation rates suggests two possibilities: that there are unrecognized diazotrophs contributing to the short-term N_2-fixation rate measurements and/or that the short-term rates are artificially high and that actual N_2-fixation rates are closer to the geochemical estimates, in particular at stations where the $\delta^{15}N$ budgets did not detect N_2 fixation. If the short-term rates are correct then the geochemical data implies that those rates do not persist for long periods of time, because the PN_{sink} flux and $\delta^{15}N$ required by the short-term rates are not consistent with the $\delta^{15}N$ budgets (Table 1).

Finally, we expect that the higher proportion of export production supported by N_2 fixation in 2011 compared with 2010 is related to the relative timing of the two cruises, with 2011 sampling later during the austral summer (March to April 2011 vs. January to February 2010). In particular, the results from a deep-moored sediment trap deployed at Station 5 from February 2010 to March 2011 records a minimum in $\delta^{15}N_{PNsink}$ between March to May 2010, when organic matter fluxes were also lowest (22), suggesting that the 2010 cruise may have preceded the peak regional significance of N_2 fixation. The deep trap results also indicate that N_2-fixation rates are unlikely to be significantly higher throughout the rest of the year, consistent with prior observations from adjacent waters sampled during the austral spring (16).

Summary

Here, we present an investigation of N_2 fixation using biological and geochemical tools to evaluate the quantitative significance of N_2 fixation in the ETSP. Although short-term N_2-fixation rates integrated over the euphotic zone averaged 60 μmol N m^{-2} d^{-1}, roughly half the rates measured in the North Pacific subtropical gyre (39), geochemical N_2-fixation rates, together with a parallel analysis of *NifH*, suggest N_2-fixation rates are lower still, from 11 to 24 μmol N m^{-2} d^{-1}, when detected at all, and play a minimal role in supporting export production. When scaled to surface waters in the South Pacific with similar nutrient characteristics (i.e., $[NO_3^- + NO_2^-] < 1.0$ μM and $[PO_4^{3-}] > 0.1$ μM; 24×10^{12} m^2), the $\delta^{15}N$ budget-based N_2-fixation rate of 10 μmol N m^{-2} d^{-1} corresponds to an annual flux of ∼1.2 Tg N y^{-1}, whereas an intermediate short-term N_2-fixation rate (or $\delta^{15}N$ budget-based rate evaluated with an alternate productivity metric) of 75 μmol N m^{-2} d^{-1} corresponds to an annual flux of 9 Tg N y^{-1}. Given that the moored trap $\delta^{15}N_{PNsink}$ data indicate that N_2-fixation fluxes are unlikely to be significantly higher throughout the rest of the year (22), 9 Tg N y^{-1} can be considered an upper bound for regional N_2-fixation fluxes. These rates are a small fraction of the 95 Tg N y^{-1} predicted for the whole Pacific basin from geochemical modeling studies (11), and also challenge the predictions (10, 11) that the highest global N_2-fixation rates are found in the Central and Eastern tropical South Pacific. This work demonstrates that low NO_3^- and relatively high PO_4^{3-} concentrations alone are insufficient to support significant N_2-fixation fluxes, perhaps because of the scarcity of iron. The findings are also consistent with recent suggestions that higher N_2-fixation rates might be found in the surface waters of the Southwest Pacific (18, 19), which maintains similarly favorable nutrient concentrations and ratios and receives relatively higher dust fluxes (15).

Materials and Methods

Water Column Sample Collection. Samples were collected on the research vessel (R/V) Atlantis in January to February 2010, and the R/V Melville in March to April 2011 on a zonal transect along 20° S between 80° W and 100° W, with exact station locations and sample depths, nutrient concentrations, and isotopic compositions reported in Table S1. Water column samples were collected by Niskin bottles deployed on a rosette equipped with conductivity temperature depth (CTD), as well as dissolved oxygen Sea-Bird Electronics sensors. All samples were collected into acid-washed, sample-rinsed high-density polyethylene bottles, and samples from the upper 400 m passed a 0.2-μm filter before collection. All samples were stored at −20 °C until analysis on land.

$NO_3^- + NO_2^-$ Concentration and Isotopic Composition Analysis. The concentration of $NO_3^- + NO_2^-$ ($[NO_3^- + NO_2^-]$) was determined using chemiluminescent analysis (44) in a configuration with a detection limit of 0.05 μM and ±0.1 μM 1 SD. The $\delta^{15}N_{NO3+NO2}$ was determined using the "denitrifier" method (45, 46) with modifications (47) on samples with $[NO_3^- + NO_2^-] > 0.3$ μM (typically ≤0.2‰ 1 SD).

Sediment Trap Sample Collection and Analysis. Sinking particulate material was collected using surface-tethered floating particle-interceptor traps (PIT) (48, 49) equipped with 12 polycarbonate cylinders. Floating sediment traps were deployed at 200 m at Stations 3 and 5 on the 2010 cruise; at all other stations traps were deployed at 100 m. Sediment trap samples were collected into a carbonate buffered brine solution and then split into replicate samples. In 2010, two splits were collected from each sediment trap, one of which was acidified to remove inorganic carbon. In 2011, two sediment traps were deployed at each station, each with an acidified and unacidified split (Table S3). In 2010, filtration through a 1-mm mesh removed "swimmers" from sediment trap material. On the 2011 cruise, swimmers were identified by dissecting microscopy and handpicked from sediment trap samples using sterilized micropipettors and forceps. Mass and isotopic fluxes were determined by combustion analysis of trap samples at the University of California Davis Stable Isotope Facility. The limit of detection for combustion analysis was 1.5 μmol of N. The mass-weighted average $\delta^{15}N$ of acidified and nonacidified splits of trap material captured in the sediment traps is reported in Table 1 and Table S3.

$^{15}N_2$-Incubation Rate Measurements. Short-term N_2-fixation rate measurements incubated with $^{15}N_2$ gas from Sigma Aldrich (lot nos. SZ1670V and MBBB0968V) were carried out in triplicate in acid-washed, sample-rinsed, light-transparent 4-L polycarbonate bottles amended with 1.5 mL of 99 atom% $^{15}N_2$ and 1.5 mL of 0.5 M $NaH^{13}CO_3$. A third batch of $^{15}N_2$ gas (Eurisotop) was used to make short-term rate measurements reported elsewhere (43). Incubations were performed with water collected from four depths within the euphotic zone under simulated in situ conditions of temperature and light and run for staggered periods (e.g., 0, 12, 24, and 48 h). Incubations were terminated by filtration of the 4-L sample onto a precombusted 25-mm Whatman glass fiber filter, which was then analyzed by mass spectrometry at the University of Southern California for $\delta^{15}N$.

The $\delta^{15}N$ of suspended particulate N (PN_{susp}) (Table S1) averaged over the upper water column (∼150 m) was used as the time zero $\delta^{15}N$ for determining the atom % excess for rate calculations. Trapezoidal integrations of discrete N_2-fixation rate measurements extended down to 150 m, except on the 2010 cruise at Station 3 (180 m) and Station 5 (175 m). Limits of detection were 10–14 μg of N, and reproducibility (±1 SD) was ±0.3‰ for $\delta^{15}N$ and ±0.1–0.2 μg for mass determinations.

Productivity Measurements. ^{234}Th-based export fluxes were reported elsewhere (37, 50), and rates of O_2/Ar-based NCP (reported in mmol C m^{-2} d^{-1}) were determined from the stoichiometric equivalent of net oxygen production (NOP) [NCP = NOP/PQ, where PQ is a photosynthetic quotient (O_2/C) taken here to have a value of 1.4 (51)]. NOP fluxes were calculated assuming steady-state O_2 mass balance within the mixed layer: $NOP = \Delta O_{2Bio} k_v O_{2eq}$ (52, 53), where k_v is piston velocity (rate of gas exchange, determined as described in ref. 54), O_{2eq} is the concentration of dissolved O_2 in equilibrium with the atmosphere at the in situ temperature and pressure, and ΔO_{2Bio} is the biological O_2 supersaturation, determined as $\Delta O_{2Bio} = O_2/Ar_{supersat} = \left(\frac{O_2/Ar_{dis}}{O_2/Ar_{eq}} - 1\right)$ to factor out the effect of temperature/salinity variability on O_2 solubility (52). The effect of bubble injection on dissolved O_2/Ar is typically small enough to be neglected (55). Additional O_2/Ar NCP methodological details are given in *SI Materials and Methods*. Finally, ^{14}C uptake and chlorophyll *a* concentration methods used the Bermuda-Atlantic Time-Series Station protocols (56).

ACKNOWLEDGMENTS. We are indebted to the efforts and expertise of the scientists and crew aboard the R/V Atlantis and R/V Melville cruises. Particular recognition goes to T. Gunderson, M. Tiahlo, and N. Rollins. This work was supported by National Science Foundation Division of Ocean Sciences (NSF-OCE) Grants 0850905 and 0850801 (to A.N.K., D.G.C., K.L.C., and W.M.B.), 0961098 (to K.L.C.), and 0961207 (to W.M.B. and M.G.P.).

1. Sigman DM, Boyle EA (2000) Glacial/interglacial variations in atmospheric carbon dioxide. *Nature* 407(6806):859–869.
2. Falkowski PG (1997) Evolution of the nitrogen cycle and its influence on the biological sequestration of CO2 in the ocean. *Nature* 387(6630):272–275.
3. Moore CM, et al. (2009) Large-scale distribution of Atlantic nitrogen fixation controlled by iron availability. *Nat Geosci* 2(12):867–871.
4. Capone DG, et al. (2005) Nitrogen fixation by Trichodesmium spp.: An important source of new nitrogen to the tropical and subtropical North Atlantic Ocean. *Global Biogeochem Cycles* 19(2):GB2024.
5. Gruber N, Sarmiento JL (1997) Global patterns of marine nitrogen fixation and denitrification. *Global Biogeochem Cycles* 11(2):235–266.
6. Brandes JA, Devol AH, Yoshinari T, Jayakumar DA, Naqvi SWA (1998) Isotopic composition of nitrate in the central Arabian Sea and eastern tropical North Pacific: A tracer for mixing and nitrogen cycles. *Limnol Oceanogr* 43(7):1680–1689.
7. Brandes JA, Devol AH (2002) A global marine-fixed nitrogen isotopic budget: Implications for Holocene nitrogen cycling. *Global Biogeochem Cycles* 16(4):1120.
8. Deutsch C, Sigman DM, Thunell RC, Meckler AN, Haug GH (2004) Isotopic constraints on glacial/interglacial changes in the oceanic nitrogen budget. *Global Biogeochem Cycles* 18(4):GB4012.
9. Eugster O, Gruber N, Deutsch C, Jaccard SL, Payne MR (2013) The dynamics of the marine nitrogen cycle across the last deglaciation. *Paleoceanography* 28(1):116–129.
10. Westberry TK, Siegel DA (2006) Spatial and temporal distribution of Trichodesmium blooms in the world's oceans. *Global Biogeochem Cycles* 20(4):GB4016.
11. Deutsch C, Sarmiento JL, Sigman DM, Gruber N, Dunne JP (2007) Spatial coupling of nitrogen inputs and losses in the ocean. *Nature* 445(7124):163–167.
12. Straub M, et al. (2013) Changes in North Atlantic nitrogen fixation controlled by ocean circulation. *Nature* 501(7466):200–203.
13. Kustka AB, et al. (2003) Iron requirements for dinitrogen- and ammonium-supported growth in cultures of Trichodesmium (IMS 101): Comparison with nitrogen fixation rates and iron: carbon ratios of field populations. *Limnol Oceanogr* 48(5):1869–1884.
14. Berman-Frank I, Cullen JT, Shaked Y, Sherrell RM, Falkowski PG (2001) Iron availability, cellular iron quotas, and nitrogen fixation in Trichodesmium. *Limnol Oceanogr* 46(6): 1249–1260.
15. Mahowald NM, et al. (2009) Atmospheric iron deposition: Global distribution, variability, and human perturbations. *Annu Rev Mar Sci* 1:245–278.
16. Bonnet S, et al. (2008) Nutrient limitation of primary productivity in the Southeast Pacific (BIOSOPE cruise). *Biogeosciences* 5(1):215–225.
17. Dutkiewicz S, Ward BA, Monteiro F, Follows MJ (2012) Interconnection of nitrogen fixers and iron in the Pacific Ocean: Theory and numerical simulations. *Global Biogeochem Cycles* 26(1):GB1012.
18. Weber T, Deutsch C (2014) Local versus basin-scale limitation of marine nitrogen fixation. *Proc Natl Acad Sci USA* 111(24):8741–8746.
19. Monteiro FM, Dutkiewicz S, Follows MJ (2011) Biogeographical controls on the marine nitrogen fixers. *Global Biogeochem Cycles* 25(2):GB2003.
20. Luo YW, et al. (2012) Database of diazotrophs in global ocean: Abundance, biomass and nitrogen fixation rates. *Earth Syst. Sci. Data* 4(1):47–73.
21. Turk-Kubo KA, Karamchandani M, Capone DG, Zehr JP (2014) The paradox of marine heterotrophic nitrogen fixation: Abundances of heterotrophic diazotrophs do not account for nitrogen fixation rates in the Eastern Tropical South Pacific. *Environ Microbiol* 16(10):3095–3114.
22. Berelson WM, et al. (2015) Biogenic particle flux and benthic remineralization in The Eastern Tropical South Pacific. *Deep Sea Res Part 1 Oceanogr Res Pap* 99:23–34.
23. Minagawa M, Wada E (1986) Nitrogen Isotope Ratios of Red Tide Organisms in the East-China-Sea - a Characterization of Biological Nitrogen-Fixation. *Mar Chem* 19(3): 245–259.
24. Carpenter EJ, Harvey HR, Fry B, Capone DG (1997) Biogeochemical tracers of the marine cyanobacterium Trichodesmium. *Deep Sea Res Part I Oceanogr Res Pap* 44(1): 27–38.
25. Sigman DM, DiFiore PJ, Hain MP, Deutsch C, Karl DM (2009) Sinking organic matter spreads the nitrogen isotope signal of pelagic denitrification in the North Pacific. *Geophys Res Lett* 36(8):L08605.
26. Altabet MA (1988) Variations in nitrogen isotopic composition between sinking and suspended particles - Implications for nitrogen cycling and particle transformation in the open ocean. *Deep Sea Res A* 35(4):535–554.
27. Knapp AN, Sigman DM, Lipschultz F (2005) N isotopic composition of dissolved organic nitrogen and nitrate at the Bermuda Atlantic time-series study site. *Global Biogeochem Cycles* 19(1):GB1018.
28. Casciotti KL, Trull TW, Glover DM, Davies D (2008) Constraints on nitrogen cycling at the subtropical North Pacific Station ALOHA from isotopic measurements of nitrate and particulate nitrogen. *Deep Sea Res Part 2 Top Stud Oceanogr* 55(14-15): 1661–1672.
29. Karsh KL, Trull TW, Lourey AJ, Sigman DM (2003) Relationship of nitrogen isotope fractionation to phytoplankton size and iron availability during the Southern Ocean Iron RElease Experiment (SOIREE). *Limnol Oceanogr* 48(3):1058–1068.
30. Granger J, Sigman DM, Needoba JA, Harrison PJ (2004) Coupled nitrogen and oxygen isotope fractionation of nitrate during assimilation by cultures of marine phytoplankton. *Limnol Oceanogr* 49(5):1763–1773.
31. Casciotti KL, Buchwald C, McIlvin M (2013) Implications of nitrate and nitrite isotopic measurements for the mechanisms of nitrogen cycling in the Peru oxygen deficient zone. *Deep Sea Res Part 1 Oceanogr Res Pap* 80:78–93.
32. Liu K-K, Kaplan IR (1989) The Eastern Tropical Pacific as a source of 15N-enriched nitrate in seawater off Southern California. *Limnol Oceanogr* 34(5):820–830.
33. Rafter PA, Sigman DM, Charles CD, Kaiser J, Haug GH (2012) Subsurface tropical Pacific nitrogen isotopic composition of nitrate: Biogeochemical signals and their transport. *Global Biogeochem Cycles* 26(1):GB1003.
34. Fawcett SE, Lomas M, Casey JR, Ward BB, Sigman DM (2011) Assimilation of upwelled nitrate by small eukaryotes in the Sargasso Sea. *Nat Geosci* 4(10):717–722.
35. Knapp AN, DiFiore PJ, Deutsch C, Sigman DM, Lipschultz F (2008) Nitrate isotopic composition between Bermuda and Puerto Rico: Implications for N(2) fixation in the Atlantic Ocean. *Global Biogeochem Cycles* 22(3):GB3014.
36. Lourey MJ, Trull TW, Sigman DM (2003) Sensitivity of delta N-15 of nitrate, surface suspended and deep sinking particulate nitrogen to seasonal nitrate depletion in the Southern Ocean. *Global Biogeochem Cycles* 17(3):1081.
37. Haskell WZ, et al. (2015) Upwelling velocity and eddy diffusivity from 7Be measurements used to compare vertical nutrient flux to export POC flux in the Eastern Tropical South Pacific. *Mar Chem* 168:140–150.
38. Emerson S (2014) Annual net community production and the biological carbon flux in the ocean. *Global Biogeochem Cycles* 28(1):14–28.
39. Sohm JA, Subramaniam A, Gunderson TE, Carpenter EJ, Capone DG (2011) Nitrogen fixation by Trichodesmium spp. and unicellular diazotrophs in the North Pacific Subtropical Gyre. *J Geophys Res Biogeosci* 116(G3):G03002.
40. Knapp AN, Sigman DM, Lipschultz F, Kustka AB, Capone DG (2011) Interbasin isotopic correspondence between upper-ocean bulk DON and subsurface nitrate and its implications for marine nitrogen cycling. *Global Biogeochem Cycles* 25(4):GB4004.
41. Dabundo R, et al. (2014) The contamination of commercial 15N2 gas stocks with 15N-labeled nitrate and ammonium and consequences for nitrogen fixation measurements. *PLoS One* 9(10):e110335.
42. Mohr W, Grosskopf T, Wallace DWR, LaRoche J (2010) Methodological underestimation of oceanic nitrogen fixation rates. *PLoS One* 5(9):e12583.
43. Dekaezemacker J, et al. (2013) Evidence of active dinitrogen fixation in surface waters of the eastern tropical South Pacific during El Niño and La Niña events and evaluation of its potential nutrient controls. *Global Biogeochem Cycles* 27(3):768–779.
44. Braman RS, Hendrix SA (1989) Nanogram nitrite and nitrate determination in environmental and biological materials by vanadium (III) reduction with chemiluminescence detection. *Anal Chem* 61(24):2715–2718.
45. Sigman DM, et al. (2001) A bacterial method for the nitrogen isotopic analysis of nitrate in seawater and freshwater. *Anal Chem* 73(17):4145–4153.
46. Casciotti KL, Sigman DM, Hastings MG, Böhlke JK, Hilkert A (2002) Measurement of the oxygen isotopic composition of nitrate in seawater and freshwater using the denitrifier method. *Anal Chem* 74(19):4905–4912.
47. McIlvin MR, Casciotti KL (2011) Technical updates to the bacterial method for nitrate isotopic analyses. *Anal Chem* 83(5):1850–1856.
48. Soutar A, Kling SA, Crill PA, Duffrin E (1977) Monitoring marine-environment through sedimentation. *Nature* 266(5598):136–139.
49. Knauer GA, Martin JH, Bruland KW (1979) Fluxes of particulate carbon, nitrogen, and phosphorus in the upper water column of the northeast Pacific. *Deep Sea Res A* 26(1): 97–108.
50. Haskell WZ, Berelson WM, Hammond DE, Capone DG (2013) Particle sinking dynamics and POC fluxes in the Eastern Tropical South Pacific based on 234Th budgets and sediment trap deployments. *Deep Sea Res Part 1 Oceanogr Res Pap* 81:1–13.
51. Laws EA (1991) Photosynthetic quotients, new production and net community production in the open ocean. *Deep Sea Res A* 38(1):143–167.
52. Emerson S, Quay P, Stump C, Wilbur D, Knox M (1991) O2, Ar, N2, and 222Rn in surface waters of the subarctic Ocean: Net biological O2 production. *Global Biogeochem Cycles* 5(1):49–69.
53. Bender M, et al. (1987) A comparison of 4 methods for determining planktonic community production. *Limnol Oceanogr* 32(5):1085–1098.
54. Yeung LY, et al. (2015) Upper-ocean gas dynamics from radon profiles in the Eastern Tropical South Pacific. *Deep Sea Res Part 1 Oceanogr Res Pap* 99:35–45.
55. Stanley RHR, Kirkpatrick JB, Cassar N, Barnett BA, Bender ML (2010) Net community production and gross primary production rates in the western equatorial Pacific. *Global Biogeochem Cycles* 24(4):GB4001.
56. Lorenzen S, Tuel M (1989) Primary production. *Bermuda Atlantic Time-Series Study* (Bermuda Biological Station for Research, St. George, Bermuda).
57. Cassar N, et al. (2009) Continuous high-frequency dissolved O2/Ar measurements by equilibrator inlet mass spectrometry. *Anal Chem* 81(5):1855–1864.